Vibration monitoring on a PC girder bridge during a bridge collapse test

Chul-Woo Kim
Professor, Dept. of Civil & Earth Engineering, Graduate School of Engineering, Kyoto University, Kyoto, Japan

Oscar Sergio Luna Vera
Ph.D., Dept. of Civil & Earth Resources Engineering, Graduate School of Engineering, Kyoto University, Kyoto, Japan

Yousuke Kondo
Graduate student, Dept. of Civil & Earth Resources Engineering, Graduate School of Engineering, Kyoto, Japan

Yoshinobu Oshima
Senior researcher, Center for Advanced Engineering Structural Assessment and Research, Public Works Research Institute, Ibaraki, Japan

ABSTRACT: Using the information gathered from structural health monitoring (SHM) has been proved successful when identifying damage on specific type of bridges. However to know the extent of the localized damage into the structural performance or even the degree of its vulnerability by means of the SHM is still under discussion. This study aims to examine how changes in load resistance capacity of an actual PC girder bridge influence on their dynamic properties. In this study a real PC girder bridge under static loadings, a bridge collapse-test, is discussed. In the static loading test, the PC Bridge was put under several loading and unloading levels until failure. Besides, forced vibration tests from both impact hammer test and moving-vehicle test were carried out along the static loading test, in order to assess the changes in the dynamic properties of the PC Bridge with different health conditions. The study investigates the influence of different phenomena, such as creep and cracks propagation, on the variation of modal parameters. Observations showed that changes in the frequency of the second bending mode was more analogous with the changes of load resistance capacity than the first bending mode.

1. INTRODUCTION

PC girder bridges have been constructed since 1970s in Japan, and in recent years, various degradations such as a corrosion of PC tendon of the PC bridge have been reported. Various methods have been proposed for evaluating the soundness of bridges, and visual inspection is one of the most popular approach to assess integrity of the PC bridge. Another approach is vibration-based structural health monitoring (SHM). The natural frequencies from deteriorated concrete girders have shown to be sensitive features for the strength reduction when evaluating the residual strength in bridges with 50 years of service life. At the same time, it rises the likelihood of using them as a symptom to be monitored in order to estimate the structural reliability (Quattrone et al. 2012). Literature has also shown that the modal damping ratio can be a damage sensitive feature for reinforced and prestressed concrete structures. Moreover, researches indicate that a trend of getting higher value of modal damping ratios with the age of the bridges could be a sign of possible

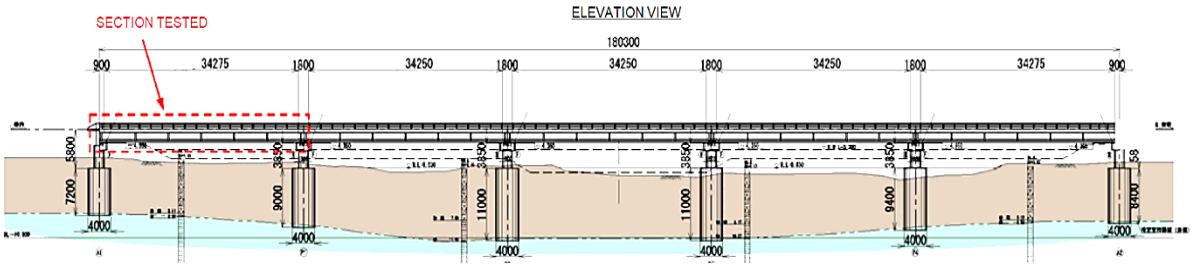

(a) General view of PC-girder bridge

(b) Loading jack for static loading test

Figure 1: Target bridge.

deterioration, which is a strong reason to investigate the relationship between damping parameter and degree of damage (Dammika et al. 2012). Regardless, more evidence is needed to validate residual strength models of deteriorating bridges (Cavell et al. 2001) and to prove the link between structural resistance and SHM by means of dynamic identification in damaged bridges (Dilena et al. 2011). Inconsistencies between experimental testing and theoretical models occur due to different reasons that need to be handled (Udwadia 2005). Damage in structures is interpreted as a decay of its mechanical properties, or in other words, a decrease in stiffness. However, the tendency of natural frequencies to the development of damage shows an abnormal increase/decrease from one configuration to another, even experimentally (Dilena et al. 2011). In a study of the failure process of a PC-bridge (Kato et al. 1986) the natural frequency of the first vertical mode has shown to decay rapidly, but little change in the damping was observed. It was noticed that the small changes in modal parameters, regardless the large presence of cracks in concrete structures, might be due to the cracks closing by effective prestressing when the structure is unloaded. The

Figure 2: Damage on girders.

Figure 3: Loading test device.

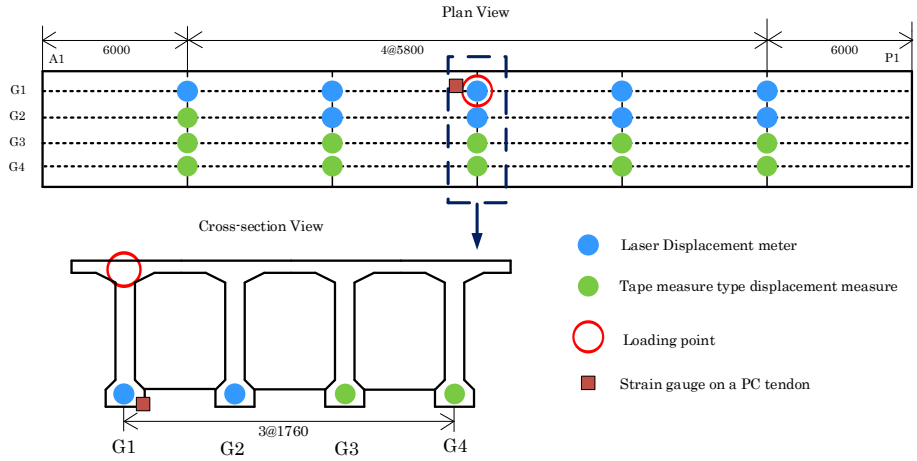

Figure 4: Observation span and location of displacement sensors.

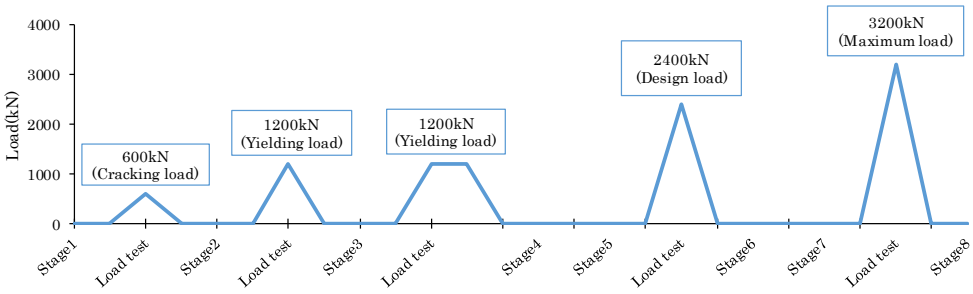

Figure 5: Loading and vibration tests history.

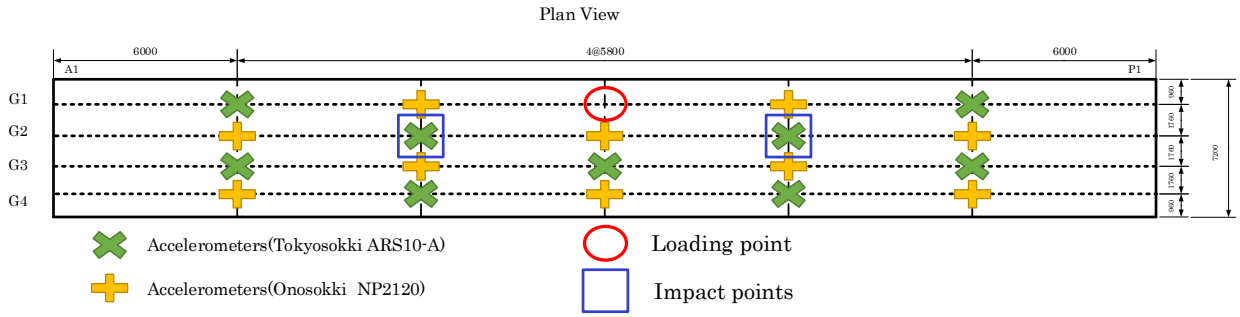

Figure 6: Location of accelerometers.

decrease of prestress force theoretically should increase the natural frequencies in a concrete element because a reduction in the axial compressive load should stiffen the element. However, an opposite trend was observed in a PC bridge under test (Saiidi et al. 1994) where the frequencies had a small decrement after the decrease of prestress force. Even more, other researches indicate that no substantial change was detected in the modal parameters after the cutting of the prestressing tendons at specific locations of a concrete bridge (Döhler et al. 2014). As a result of the previous literature review, this study discusses a bridge collapse test under static loading on a real PC girder bridge. In the static loading test, several loading and unloading levels until failure were considered. In addition, forced vibration tests were carried out along with the static loading test in order to estimate the relationships between modal parameters and structural performance.

2. STATIC LOADING AND VIBRATION TESTS

2.1. Target bridge

The target bridge consists of four PC girders and five spans. The length of each span is 34.3 meters and width of 7.2 meters. One span of them is the target of the experiment. Figure 1 shows the target bridge with the static loading device installed. The bridge had been operated more than 50 years since its construction. The bridge suffered salt damage to the main girder, and cracks in the main girder and peelings of the concrete caused by corrosion of internal steel material were observed by visual inspection. Figure 2 shows the appearance of the lower part of the girder, in which cracks in the longitudinal direction, exposed reinforcing steel and peeling of repair/reinforcing material can be observed.

2.2. Static loading test

The static loading test was carried out by means of a single point load from two jacks which have a capacity of 2500kN per each. Figure 3 shows the loading test device. The load point is set at the span center of the outer girder (G1 girder in Figure 4), and static load was monotonically increased. Twenty displacement sensors were distributed uniformly under the girders, five in each girder as shown in Figure 4. From these twenty sensors, nine displacement sensors were laser type (mostly allocated under girder G1 and G2) and the other eleven were displacement transducers of tape measure type.

The test was carried out over three days. A stepwise repeated loading was applied until the upper flange of the loading girder collapsed, which is the assumed ultimate condition. However, wheel guards were collapsed due to increase the compressive force at the top of the girder before the ultimate condition, and the static loading test had been completely stopped due to this collapse. Figure 5 shows the loading history, including the stages of the vibration test which are described in the next section. The horizontal axis indicates test stages progressed during the three days. 600kN, 1200kN, 2400kN and 3200kN respectively indicate cracking load, yielding load, design load and maximum load.

2.3. Vibration test

Two kinds of vibration tests were carried out at each stage shown in Figure 5 in order to assess the changes in the dynamic properties with different loading conditions.

2.3.1. Moving-vehicle test

The moving-vehicle test is an output-only technique in which vibrations of the PC-bridge are produced by the pass of a vehicle over the bridge. In each stage, moving-vehicle test was conducted. Strain type accelerometers (ARS-10A, Tokyo Sokki) were used during the moving-vehicle test. The location of accelerometers is shown in Figure 6. As a test vehicle, a heavy vehicle is desirable as it is expected to provide greater excitation force. However, a smaller vehicle, van type vehicle (HIACE, Toyota Motor Corporation), was used because of the restriction of the vehicle passageway due to the static loading device on the bridge. The speed was approximately 30km/h. Three runs for stage 1, and five runs for other stages were carried out.

2.3.2. Impact-hammer test

In each stage, the impact-hammer test was conducted as identification accuracy of vibration characteristics by the impact-hammer test is better than that by moving-vehicle test. The equipment used for this test consists of an impact hammer Brüel & Kjær type 8210 – Modal sledge hammer 12-pound head with a maximum compressive force of 44.4 kN and a sensitivity of 0.225 mV/N. Piezoelectric type accelerometers (NP2120, Ono Sokki) were used during the impact hammer test. The impact roving technique was used to obtain the transfer function matrix, where two impact points on the top surface of the bridge were considered as shown in Figure 6. In each stage, the bridge was hit 10 times in each impact point by using two different types of impact tip (medium and tough tips), and the total hitting times was 40 per each stage.

3. RESULT OF STATIC LOADING AND VIBRATION TEST

3.1. Load-displacement relation

Figure 7 shows the load-displacement curve observed at the span center of the G1 girder. No clear residual displacement was observed until stage 4 where the yield of an outermost rebar was observed. It indicates the bridge behaviour is elastic. After stage 5, the bridge was loaded up to 2500kN, which is the maximum design load, and unloaded. The maximum design load resulted in the residual displacement of around 16mm. Moreover, when the bridge is reloaded, the load-displacement curve traces the unloading point (point A, Figure 7), which shows the possession of enough restoration force. The gradient of reloading was almost the same as that of the stages 1 to 3 until the tension is generated at the lower edge of the concrete. This proved that the prestressed force remains in order to keep the entire section effective. Therefore, when the load level is low, it can be said that the vibration characteristics are hardly changed as the initial stiffness was about the same as those of stage 1 to 3.

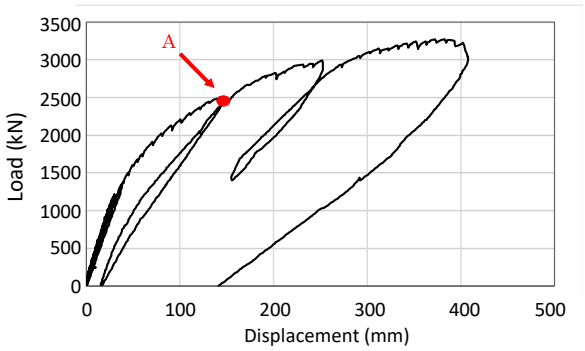

Figure 7: Load vs. displacement curve.

3.2. Load-strain relation

Figure 8 shows the load-strain curve observed at near the span center of the G1 girder (see Figure 4). From the Figure 8, it is clear that the rupture of the PC tendon occurs when around 2700kN load is given.

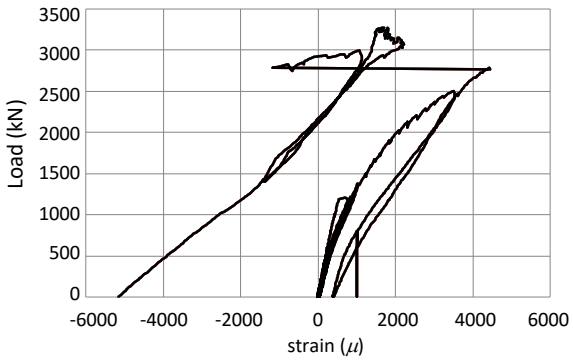

Figure 8: Load vs. strain curve.

3.3. Energy-based asymmetric bending performance

The static load applied to the PC-bridge produced an unbalanced effect into the system response. A way to measure this asymmetric bending performance is by calculating the energy dissipation and potential energy in each load-unload step. These energy concepts are shown graphically in Figure 9 where the enclosed area in the load-displacement graph is the energy dissipation (ΔW) and the potential energy, or work applied (W), is the area below the curve in the same graph, but this time considering only the loading process. The energy capacity Z can be defined as Eq. (1) in order to calculate the global bending performance.

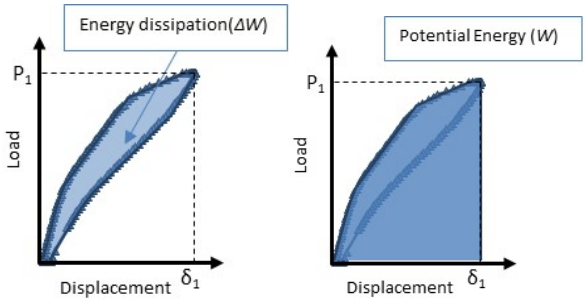

(a) Energy dissipation (b) Potential energy

Figure 9: Energy dissipation and potential energy.

$$Z = \left(1 - \frac{\Delta W}{W}\right) \times 100 \qquad (1)$$

This performance describes the behavior of the bridge under asymmetric bending and it decreases when the energy dissipation is inversely increased. Figure 10 shows the change in the

performance with respect to each stage. From Figure 10, the value of the energy capacity abruptly decreases due to the loading larger than the yielding load.

3.4. Residual displacement

The residual displacement is an effective parameter for evaluating the restoring force of the PC tendon. Figure11 shows the change in the amount of the remained displacement area at each stage with the displacements in the initial state as the reference. The remained displacement area is estimated from the area of the uncovered elastic curve of the PC bridge due to residual displacement of each observation point. From Figure 11, the remained displacement area increases acceleratively after yielding. Also, in stages 3 and 4, the remained displacement area shows a negative value, which means that the residual displacement of each observation point was upward in the vertical direction. Although this cause cannot be clarified, it seems to be related to the time dependent behavior of concrete.

3.5. Natural frequency and damping ratio

This study focuses on the natural frequency and damping ratio as one of the representative vibration characteristics. Vibration characteristics are identified by using stochastic subspace identification (SSI) (Overschee et al. 1996) for the acceleration response obtained from moving-vehicle test. For the impact hammer-test, vibration characteristics were identified by using the frequency response function. Figure 12 and Figure 13 show the change in natural frequency corresponding to the 1st and 2nd bending modes. From two figures, the natural frequency for the 2nd bending mode obtained from impact-hammer test resulted in stronger relationship with structural integrity. The precision of the natural frequency identified from moving-vehicle test was poor due to the weak excitation.

Figure 14 and Figure 15 shows the change in damping ratio corresponding to the 1st and 2nd bending modes. In previous study (Miyanaga et al. 2013), the decrease of the prestressed force makes damping ratio increase. In this experiment,

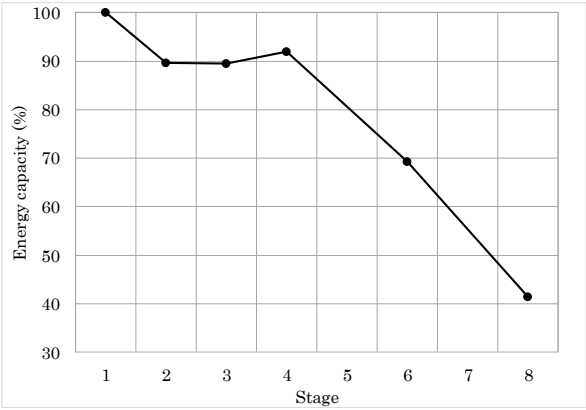

Figure 10: Change in energy capacity w.r.t. loading stages.

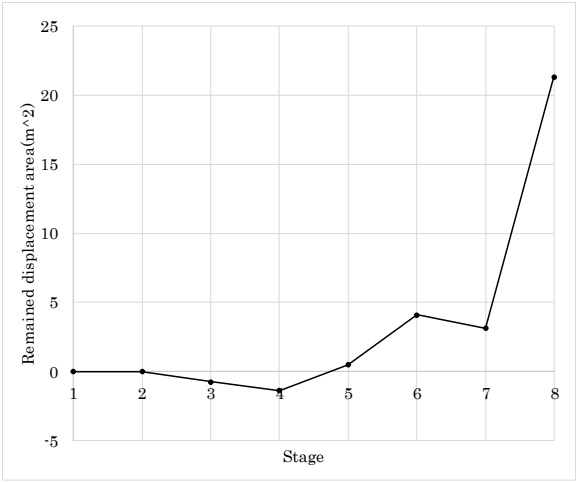

Figure 11: Change in remained displacement area w.r.t. loading stages.

the rupture of the PC tendon is confirmed at stage8, and the damping ratio of 2nd bending mode greatly increases as shown in Figure 15. Therefore, this resulted 2nd bending mode has stronger relationship with structural integrity.

3.6. Energy capacity and natural frequency

The comparisons of changes in energy capacity and changes in natural frequency are shown in Figure 16, which shows a linear regression between frequency and energy capacity from stage 1 to stage 7. Stage 8 was not considered to the regression since stage 8 is close to the ultimate condition. From the linear regression, it is observed a correlation between the 2nd bending modal frequency and the energy capacity.

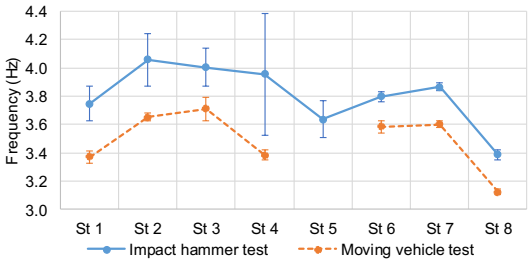

Figure 12: Change in 1st bending modal frequency.

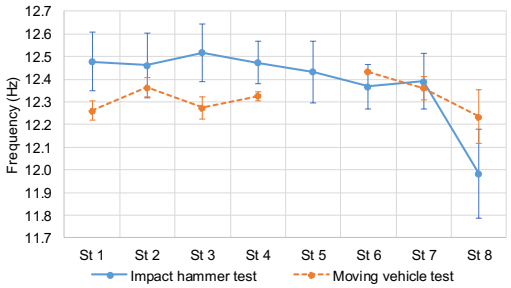

Figure 13: Change in 2nd bending modal frequency.

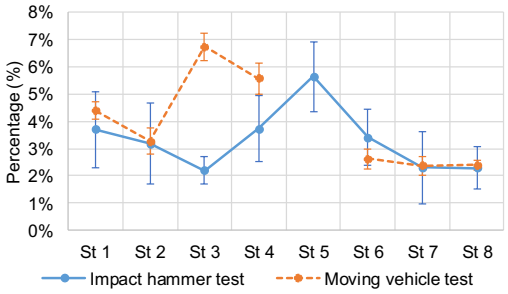

Figure 14: Change in 1st bending modal damping ratio.

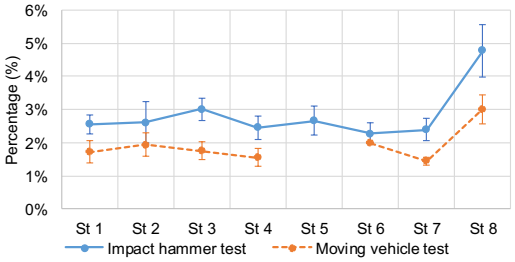

Figure 15: Change in 2nd bending modal damping ratio.

3.7. Residual displacement and natural frequency

Figure 17 shows the comparison of changes in residual displacement and changes in natural frequency. The dotted line in the figure shows a

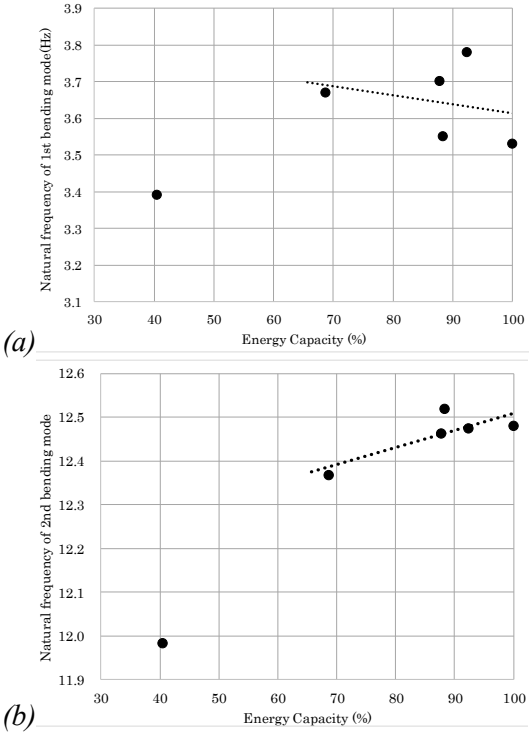

Figure 16: Energy capacity vs. frequency: (a) 1st bending mode; (b) 2nd bending mode.

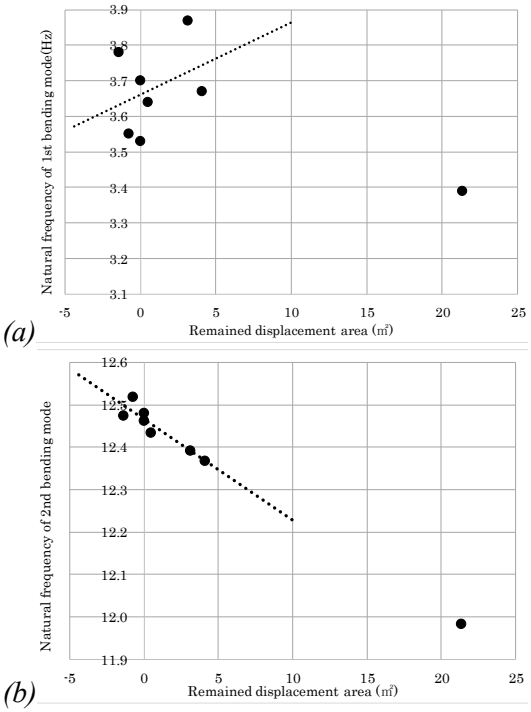

Figure 17: Remained displacement area vs. frequency: (a) 1st bending mode; (b) 2nd bending mode.

linear regression between them from stage 1 to stage 8. From the linear regression, 2nd bending modal frequency has a correlation with residual displacement, and this correlation is stronger than that between energy capacity and natural frequency.

4. CONCLUSIONS

This study tackles the relationship between bridge performance and modal parameter. In regards to natural frequency, the 2nd bending mode showed stronger correlation with energy capacity and remained displacement area than the 1st bending mode. This result is similar to the PC girder damage experiment in laboratory (Luna Vera et. al. 2017), and indicates the usefulness of the 2nd bending mode in vibration-based bridge health monitoring of PC bridges.

As a next step for this research, comprehensive investigations on structural performance of the PC bridge will be carried out utilizing strains measured at concrete and rebars, and effectiveness of the correlation between the bridge performance and vibration characteristics will be investigated by numerical analysis. Then, numerical analysis will be carried out by creating the model of the target bridge in order to confirm the validity of the relationship between bridge performance and modal parameter. Finally, by using the model high in reproducibility, we will investigate the difference by the change in the location and the type of damages.

5. REFERENCES

Quattrone, A., Matta, E., Zanotti Fragonara, L., Ceravolo, R. and De Stefano, A. (2012) "Vibration tests on dismounted bridge beams and effects of deterioration," J. of Physics: Conference Series 382.

Dammika, A. J., Sheharyar, R., Takanami, R., Yamaguchi, H. and Matsumoto, Y. (2015). "An investigation on modal damping ratio as an indicator of invisible damage in PC bridges," in Proc. Int. Symp. on Life-Cycle Civil Engineering, London.

Cavell, D. and Waldron, P. (2001). "A residual strength model for deteriorating post-tensioned concrete bridges," Computers and Structures, 79: 361-373.

Dilena, M., Morassi, A. and Perin, M. (2011). "Dynamic identification of a reinforced concrete damaged bridge," Mechanical Systems and Signal Processing, 25: 2990-3009.

Udwadia, F.E. (2005). "Structural Identification and Damage Detection from Noisy Modal Data," Journal of Aerospace Engineering, 18(3): 179-187.

Dilena, M. and Morassi, A. (2011). "Dynamic testing of a damaged bridge," Mechanical Systems and Signal Processing, 25(5): 1485-1507.

Kato, M. and Shimada, S. (1986). "Vibration of PC Bridge during Failure Process," Journal of Structural Engineering, 112(7): 1692-1703.

Saiidi, M., Douglas, B. and Feng, S. (1994). "Prestress Force Effect on Vibration Frequency of Concrete Bridges," Journal of Structural Engineering, 120(7): 2233-2241.

Döhler, M., Hille, F., Mevel, L. and Rücker, W. (2014). "Structural health monitoring with statistical methods during progressive damage test of S101 Bridge," Engineering Structures, 69: 183-193.

Miyanaga, K., Aoki, K. and Nojima, S. (2013). "Monitoring of vibration characteristics of PC bridge and a rupture of PC tendon," Japan Prestressed Concrete Institute, 22nd Symposium: 353-358.

van Overschee, P. and De Moor, B. (1996) "Subspace Identification for linear Systems," Boston/London/Dordrecht: Kluwer Academic Publishers.

Luna Vera, O.S., Kim, C.W. and Oshima, Y. (2017). "Energy dissipation and absorption capacity influence on modal parameters of a PC girder", J. of Physics: Conf. series 842.